Radar sea echo in UHF in coastal zone: experimental observations and theory

P. Forget[(1)], Y. Barbin[(1)], P. Currier[(2)] and M. Saillard[(2)]

[(1)] LSEET, CNRS/Université de Toulon et du Var, bp132, 83957 La Garde cedex, France
[(3)] Etablissement Degréane Electronique, 28 Avenue de Font-Pré, bp621, 83053 Toulon cedex, France
[(4)] Institut Fresnel, DU St-Jérôme, 13397, Marseille cedex 20, France

***Abstract* - We present the results of a preliminary experiment of remote sensing of near-shore environment by an UHF radar initially devoted to atmospheric wind profiling. VV and HH Doppler signatures of the sea surface during a one-day experiment are analyzed in terms of signal decay with distance and Doppler spectra morphology. Marked differences between VV ("slow" scatterers) and HH spectra ("fast" scatterers) were observed. VV spectra could be partly reproduced considering a first-order Bragg theory.**

I. INTRODUCTION

L-band radar is a central technique for many oceanographic satellites. However the direct use of land-based coherent UHF radars for sensing near-shore environment in terms of wave and current characteristics has been rarely tempted. The main advantages of the UHF technique for that goal is the fine spatial resolution and the short distances from the shore line that it can provide. From these points of view, UHF radars could come in complement to HF/VHF radars often used in coastal oceanography. We initiated a program for assessing the technique and here are preliminary results at low grazing angle and relatively high sea state conditions.

II. EXPERIMENTAL CONDITIONS .

A one-day experiment was conducted in December 2002 using a coherent pulsed UHF radar designed and manufactured by Etablissement Degréane Electronique and primarily dedicated to wind speed and turbulence measurements in the troposphere. Basically the antenna system consists of 5 identical antennas pointing vertically and obliquely but here only one of them was used (Fig. 1). It consists of an array of 8x8 parallel dipoles disposed over a metallic panel, the dipole axis being parallel to the plane of the panel. The plane of the antenna was disposed vertically in order to point to the sea. Given the geometry the grazing angles are very low, from α=2.18° (x=100m) to α=0.05° (x=4000m). Two configurations were achieved to get signals at polarizations VV (dipole axis in vertical position, from 11:30 to 14:35) and HH (horizontal position after a 90° rotation of the antenna in the vertical plane, from 15:00 to 16:15). The horizontal 3dB beam width was 8°4 in VV (first side lobes at ±13°, rejection 17dB) and 10°.0 in HH (±15°, 14dB).

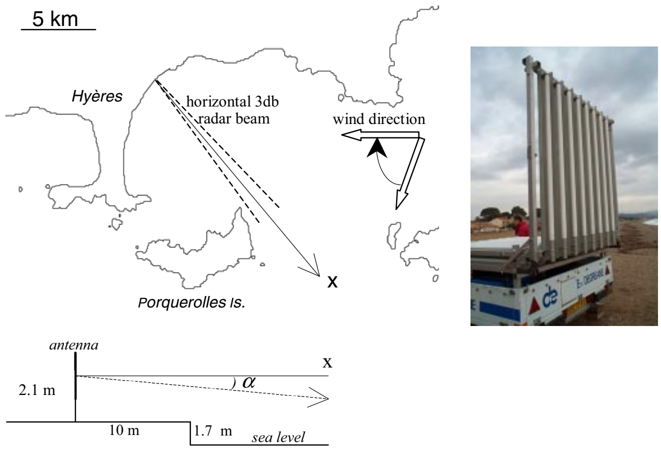

Figure 1. Experimental conditions

The typical radar and data processing characteristics are given in Table 1. Doppler spectra of 128 points were computed from radar signals. The temporal series exhibit slow variations of the general characteristics of these spectra. Without loosing information we could increase, by summation of the spectra, the number of degrees of freedom of spectral amplitudes, initially of the order of 20 (Table 1), up to 400. The final data set then consists of 21 sets of Doppler spectra, 10 in VV and 11 in HH.

The wind regime varied from the N/NE sector (6 knots, 11:00 to 12:00) to the E sector (7-18 knots).

III. POWER CONSIDERATIONS

Variation with distance. Fig. 2 shows a typical variation of the backscattered power, P_R , with distance x. Saturation is observed is the first kilometer and P_R decreases in x^a for 1400m<x<5000m. A mean value a=-5.95 (sd=0.09) was obtained in VV and a=-5.48 (sd=0.36) in HH. a, of the order of -6, is much smaller than the value of -3 which is expected

TABLE I

MAIN RADAR AND (TYPICAL) DATA PROCESSING CHARACTERISTICS

Frequency	1.238 GHz
Peak power	4000 W
Pulse width	0.5 µs
Number of coherent summation	75 (VV) , 25 (HH)
Number of incoherent summation	20
range sampling, range spacing	100-7000 m , 60 m

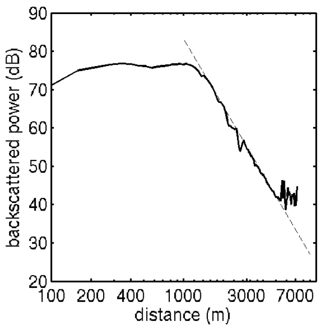

Figure 2. Variation with distance of the backscattered power in VV.

from the radar equation [1]. The variations of the backscattering coefficient, σ^0, with grazing incidence angle and thus with distance could support part of the extra x^{-3} variation observed. Theoretical arguments can be found in, e.g., Barrick [2]. We plan to go further in the investigation of that hypothesis.

Maximum-minimum ranges. In present conditions of noise and system performances the maximum range achievable, x_{max} , was around 5000m both in VV and HH and the minimum (unsaturated) range, x_{min} , was 1400m in VV and 1100m in HH. Considering the decay rates a above, and considering a same transmitted power, the interval x_{min}-x_{max} could be shifted to lower values for near-shore observation by attenuating the transmit power but the interval would be reduced. For example, a 30dB (50dB) attenuation gives x_{min}-x_{max}=440-1570m (200-700m) in VV.

IV. Doppler spectra

Figure 3 provides a velocity-distance view of 2 series of Doppler spectra (VV and HH) and, for each of them, an individual spectrum including the position of the Bragg waves velocities ($\pm V_B$ with V_B=0.43 m.s^{-1}). Spurious echoes are observed due to strong scatterers detected by the antenna side lobes: the boats of a harbor (vicinity of 2500m-0m.s^{-1}) and, in addition, in HH, cars and other vehicles (red spots).

The spectra for the first cells were computed from saturated signals (Fig. 2). They present a triangular shape and the noise level is higher that for non-saturated signals (Fig. 4). These aspects were correctly simulated by modeling the radar signal corresponding to a non-saturated spectrum and saturating this signal according to the range variations observed above. Saturation seems to preserve the position of the peak

VV sea echo Doppler spectra are generally single-peaked with a velocity of the maximum, V_{max}, varying from 0.8 to 1 m.s^{-1}. These values are close to V_B and this strongly suggests that the main interacting process between e.m. waves and the sea surface is of Bragg type. We will try to model the spectra on the basis of this hypothesis in the next section. One part of the difference V_{max}-V_B could be due, in present conditions of relatively strong wind, to the surface current generated by the wind, the magnitude of which is generally of the order of a few percent of the wind speed.

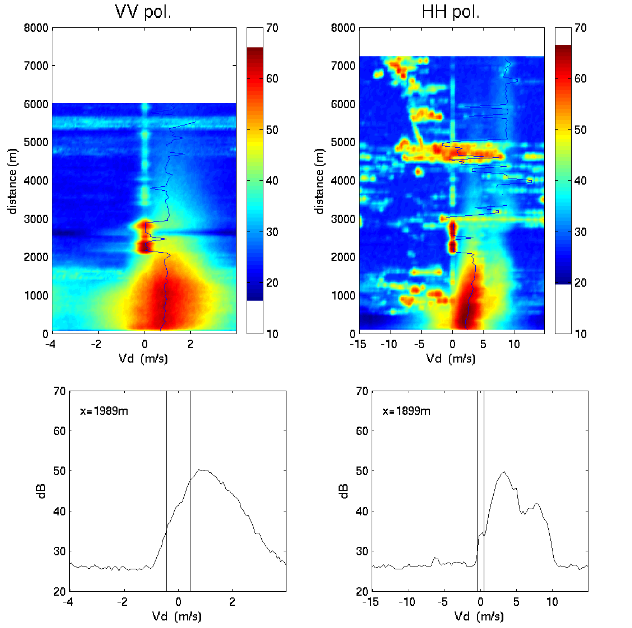

Figure 3. Upper: variation with distance of the Doppler spectra (V_d: Doppler velocity). Lower: typical spectra (vertical lines: Bragg frequencies).

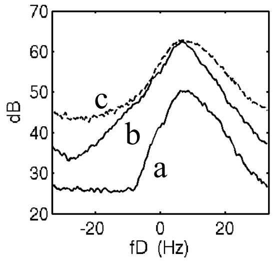

Figure 4. Saturation effects. Doppler spectra for unsaturated (a) and saturated (b) radar signals. (c): simulation of (b).

HH spectra are generally double-peaked, the maximum of the first one, (P1), increasing offshore from 3.2 to 4 m.s^{-1} and that of the second peak, (P2), from 6.7 to 8.7 m.s^{-1}.

The velocities associated to (P1), V_1 , are intermediate between V_B and the velocity of the dominant waves, V_m, estimated greater than 6 m.s^{-1} or so. Our data in VV and in HH for (P1) are very consistent to those of Lee et al. (and others) in X band [3] who observed that VV spectra were dominated by the "slow" peak associated to Bragg waves propagating on a current whereas HH spectra were dominated by the "fast" peak associated to longer waves, not necessary the dominant waves. No measurements of wave peak frequency and direction was available in our case. We just noticed that the values of V_1 were roughly consistent with the velocity of a dominant wave of frequency $F_m \approx 0.19$ Hz traveling at an angle φ=-117° with respect to the direction of observation. The value of F_m was found by resolving at every distance for the mean values of V_1 over the radar vacations the equation of conservation of gravity wave period writing here as:

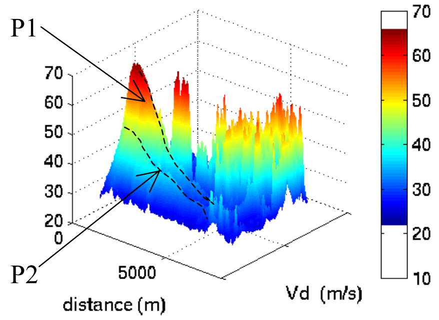

Figure 5. HH Doppler spectra showing the different decrease rate of peaks (P1) and (P2)

$$2\pi F_m(V_1 / \cos\varphi) = g \tanh\left[2\pi F_m h / (V_1 / \cos\varphi)\right] \quad (1)$$

where h is the water depth (varying from 8 to 25m) and g the gravity acceleration. These values for F_m and φ are coherent with the wind conditions encountered suggesting that the spectral peak (P1) is mainly due to the dominant waves, as found in some laboratory experiments [4].

The peak (P2) in HH is an original observation. The corresponding velocity values are also consistent with the dominant waves expected above but, given the geometry of the experiment (Fig. 1), these waves would be detected along a side-lobe. An interesting feature of (P2) can be seen on Fig. 5: its amplitude decrease rate is smaller than that of peak (P1). We have no explanation for that.

V. MODELING THE DOPPLER SPECTRA IN VV

The model assumes that Bragg scatter is responsible for the radar echo in VV. At every location $\boldsymbol{x}$ within the radar cell the Bragg wave energy is modulated by long waves according to the weak hydrodynamic wave-wave interaction theory often used in SAR studies of ocean waves [5] and is Doppler shifted by the horizontal components of the orbital velocities and accelerations imparted by surface waves. The modeling process consists in generating a realistic sea surface (random phases, given wave spectrum $\Psi(\boldsymbol{k})$), the corresponding modulation $m(\boldsymbol{x})$ of the backscattering coefficient and the surface field of Doppler frequencies. The Doppler spectrum is computed by summation in prescribed frequency bands of the contributions from the pixels presenting the same Doppler shifts. A similar approach was performed by Plant and Keller [6].

One result is shown on Fig. 6. We considered a Pierson-Moskowitz spectrum, a cardioidal angular distribution of wave energy around the wind direction, a wind speed W=7 m/s and direction φ_W=-150° and a radial approaching current of velocity U=0.5 m.s^{-1}. Other wave spectra and wind parameters were also used giving similar results as in Fig. 6. Our simple model reproduces quite well the continuum on the left side of the peak. The positive slope depends essentially on φ_W and on the model for the angular distribution of wave

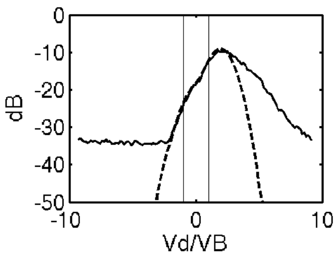

Figure 6. VV Doppler spectrum modelisation : experimental spectrum (solid line), model (dashed line).

energy. The model underestimates the energy on the right side of the peak suggesting higher-order hydrodynamic and electromagnetic effects as be seen also in [3].

We also tested the popular model of Barrick [7]. The model gives second-order narrow peaks centered on the Bragg lines. Clearly, our conditions of high sea state violate the limits of validity of Barrick's theory which then cannot be applied.

VI. CONCLUSION

A test UHF experiment was performed at very low grazing angle in conditions of relatively high sea state. The results confirm many aspects that can be found in literature concerning the sea Doppler signatures in HH and VV. In particular the VV spectra exhibit a main contribution from "low" scatterers (the Bragg waves) and the HH spectra "fast" scatterers (with velocities of the order of dominant waves velocities). The first effect was quite satisfactorily modeled while the second one manifestly needs an other theoretical approach. Interesting observations could be done considering the propagation loss. We now plan an elevated short test experiment and a longer experiment with in situ measurements of wind, waves and currents which is necessary to explore the technique for coastal oceanography.

REFERENCES

[1] M.I. Skolnik, *Introduction to radar systems*, Mc Graw Hill, p. 472, 1980.

[2] D.E. Barrick, "Grazing behavior of scatter and propagation above any rough surface", *IEEE Trans. Antennas Propagat.*, vol. 46, no1, pp. 73-83, 1998.

[3] P.H. Lee, J.D. Barter, K.L. Beach, C.L. Hindman, B.M. Lake, H. Rungaldier, J.C. Shelton, A.B. Williams, R. Yee, and H.C. Yuen, "X band microwave backscattering from ocean waves", *J. Geophys. Res.*, vol. 100, pp. 2591-2611, 1995.

[4] N. Ebuchi, H. Kawamura and Y. Toba, "Physical processes of microwave backscattering from laboratory wind wave surfaces", *J. Geophys. Res.*, vol. 98, pp. 14669-681, 1993.

[5] K. Hasselmann and S. Hasselmann, "On the nonlinear mapping of an ocean wave spectrum into a synthetic aperture radar image spectrum and its inversion", *J. Geophys. Res.*, vol. 96, C6, pp. 10713-729, 1991.

[6] W.J. Plant and W. Keller, "Evidence of Bragg scattering in microwave Doppler spectra of sea return", *J. Geophys. Res.*, vol. 95, pp. 16299-310, 1990.

[7] D.E. Barrick, "Remote sensing of sea state by radar", *Remote Sensing of the Troposphere*, V.E. Derr, Ed., U.S. Gov. Printing Office, Washington, D.C., Chap. 12, 1972.